Detectability of Chlorofluorocarbons in the Atmospheres of Habitable M-dwarf Planets

Jacob Haqq-Misra[1] , Ravi Kopparapu[2,3] , Thomas J. Fauchez[2,3,4,5] , Adam Frank[6], Jason T. Wright[7,8,9] , and
Manasvi Lingam[10]

[1] Blue Marble Space Institute of Science, Seattle, WA, USA; jacob@bmsis.org
[2] NASA Goddard Space Flight Center, 8800 Greenbelt Road, Greenbelt, MD 20771, USA
[3] Sellers Exoplanet Environment Collaboration (SEEC), NASA Goddard Space Flight Center
[4] Goddard Earth Sciences Technology and Research (GESTAR), Universities Space Research Association, Columbia, MD, USA
[5] American University, Washington DC, USA
[6] Department of Physics and Astronomy, University of Rochester, Rochester, NY, 14620, USA
[7] Department of Astronomy & Astrophysics, The Pennsylvania State University, University Park, PA, 16802, USA
[8] Center for Exoplanets and Habitable Worlds, The Pennsylvania State University, University Park, PA, 16802, USA
[9] Penn State Extraterrestrial Intelligence Center, The Pennsylvania State University, University Park, PA, 16802, USA
[10] Department of Aerospace, Physics and Space Sciences, Florida Institute of Technology, Melbourne, FL 32901, USA
Received 2021 May 24; revised 2022 February 3; accepted 2022 February 9; published 2022 March 9

Abstract

The presence of chlorofluorocarbons (CFCs) in Earth's atmosphere is a direct result of technology. Ozone-depleting CFCs have been banned by most countries, but some CFCs have persisted in elevated concentrations due to their long stratospheric lifetimes. CFCs are effective greenhouse gases and could serve as a remotely detectable spectral signature of technology. Here we use a three-dimensional climate model and a synthetic spectrum generator to assess the detectability of CFC-11 and CFC-12 as a technosignature on exoplanets. We consider the case of TRAPPIST-1e as well as a habitable Earth-like planet around a 3300 K M-dwarf star, with CFC abundances ranging from one to five times of present-day levels. Assuming an optimistic James Webb Space Telescope (JWST) Mid-Infrared Instrument low-resolution spectrometer noise floor level of 10 ppm to multiple coadded observations, we find that spectral features potentially attributable to present or historic Earth-level CFC features could be detected with a signal-to-noise ratio ⩾3–5 on TRAPPIST-1e, if present, in ∼100 hr of in-transit time. However, applying a very conservative 50 ppm noise floor to coadded observations, even a five times Earth-level CFC would not be detectable regardless of the observation time. Such observations could be carried out simultaneously and at no additional cost with searches for biosignature gases. Nondetection would place upper limits on the CFC concentration. We find that with the launch of the JWST, humanity may be approaching the cusp of being able to detect passive atmospheric technosignatures equal in strength to its own around the nearest stars.

1. Introduction

Thousands of exoplanets have so far been discovered from space-based telescopes, such as Kepler and TESS, as well as from ground-based observatories. Detection methods can constrain the orbital position and bulk properties of such planets, but follow-up observations of planetary spectra in transit, emitted, or reflected light can provide information about the presence and composition of a planet's atmosphere. These methods have already been demonstrated for the spectral characterization of gas giant atmospheres (e.g., Charbonneau et al. 2002; Benneke et al. 2019; Tsiaras et al. 2019), while detecting and characterizing the atmospheres of smaller, Earth-sized planets remains an ongoing priority for exoplanet science.

One of the astrobiological motivations for the spectral characterization of planetary atmospheres is the possibility of detecting evidence of life on an exoplanet. This has inspired the search for "biosignatures," which refer to remotely detectable spectral features that could indicate evidence of life on an exoplanet. The idea of searching for spectral biosignatures has received significant attention with regard to identifying plausible biosignatures, assessing their detectability limits, and developing strategies for conducting a search for them in

tandem with the broader goals of the astrophysics community (e.g., Seager et al. 2012; Grenfell 2017; Kaltenegger 2017; Catling et al. 2018; Fujii et al. 2018; Meadows et al. 2018; Schwieterman et al. 2018; Walker et al. 2018; Lammer et al. 2019; O'Malley-James & Kaltenegger 2019).

Biosignatures refer generally to any remotely detectable evidence of life, while "technosignatures" (Tarter 2007) specifically describe observational evidence of technology that could be detected through astronomical means. Technosignatures are a logical continuation of the search for biosignatures, both of which draw upon the history of life and technology on Earth as examples of planetary evolution (NASA Technosignatures Workshop Participants 2018). The science of identifying and classifying technosignatures, and developing cost-efficient methods to search for them, remains in a state of infancy compared to biosignature science (Wright 2019; Haqq-Misra et al. 2020; Lingam & Loeb 2021). Nevertheless, several possible classes of technosignatures have already been identified that include waste heat (Dyson 1960; Carrigan 2009; Wright et al. 2014; Kuhn & Berdyugina 2015), artificial illumination (Schneider et al. 2010; Loeb & Turner 2012; Kipping & Teachey 2016; Tabor & Loeb 2021), artificial atmospheric constituents (Owen 1980; Campbell 2006; Schneider et al. 2010; Lin et al. 2014; Stevens et al. 2016; Kopparapu et al. 2021), artificial surface constituents (Lingam & Loeb 2017), stellar pollution (Shklovskii & Sagan 1966; Whitmire & Wright 1980; Stevens et al. 2016), nonterrestrial artifacts (Bracewell 1960; Freitas Jr & Valdes 1980; Rose &

Wright 2004; Haqq-Misra & Kopparapu 2012), and mega-structures (Dyson 1960; Arnold 2005; Forgan 2013; Wright et al. 2016).

The modern era of SETI (Wright et al. 2018; i.e., the search for technosignatures) began with the realization that humanity could use existing technology to detect a similar level of technology over interstellar distances (Cocconi & Morrison 1959; i.e., powerful, deliberately directed radio signals). A major milestone in SETI would be achieved when present-day detection technologies become sensitive enough to detect humanity's ongoing and passive technosignatures at such distances. The full Square Kilometer Array, for instance, is thought to be sensitive enough to detect humanity's typical radar emission at distances of a few parsecs (Loeb & Zaldarriaga 2007); however, future projections in which Earth's radio leakage decreases significantly would be much more difficult to detect (Forgan & Nichol 2011).

Industrial pollution represents a class of atmospheric constituents on Earth that could conceivably be technosignatures if observed in the spectra of an exoplanet. One example is nitrogen dioxide (NO_2), which has large sources on Earth from combustion that are greater than nonanthropogenic sources. A study by Kopparapu et al. (2021) showed that the absorption features of NO_2 in the 0.2–0.7 μm range could be detectable with the Large Ultraviolet Optical IR Surveyor (LUVOIR; LUVOIR Team 2019). Kopparapu et al. (2021) found that a 15 m LUVOIR-like telescope could detect Earth-like levels of NO_2 for a planet around a Sun-like star with ~400 hr of observation, while planets orbiting K-dwarf stars would require even less time due to the reduction in loss of NO_2 from photolysis in such systems. The detection of elevated NO_2 levels in the atmosphere of an exoplanet could be consistent with ongoing industrial processes on the surface, although any such observations would need to be evaluated against possible nontechnological explanations before concluding that the NO_2 must be a technosignature. In this regard, such a search for technosignatures shares the same ambiguity or tentative nature as many or most searches for biosignatures.

In this study, we examine halocarbons—molecules that contain carbon and halogen atoms—as another class of pollutants that could serve as technosignatures. We specifically focus on chlorofluorocarbons (CFCs), which are only produced in significant quantities on Earth from industrial uses as refrigerants, blowing agents, and cleaning agents. CFCs are potent greenhouse agents with long atmospheric residence times. The only sink for most CFCs is photolysis by ultraviolet radiation in the stratosphere, which releases chlorine atoms that cause the depletion of stratospheric ozone on Earth (Seinfeld & Pandis 2006). The Montreal Protocol of 1987 placed limits on the production of certain CFCs in order to prevent further damage to the ozone layer (Velders et al. 2007). These provisions have been successful to the extent that ozone-depleting compounds are much less present in the stratosphere; however, the recovery of the ozone layer to pre-1980s levels appears to be slow and shows large uncertainties in both measurements and model projections (e.g., Eyring et al. 2010; Chipperfield et al. 2017).

Observing CFCs in the atmosphere of an exoplanet would be compelling evidence of a technosignature. The accumulation of CFCs on an exoplanet could be the result of ongoing industrial processes (Owen 1980; Campbell 2006; Schneider et al. 2010), particularly for a planet on which ozone loss is not a concern.

CFCs could also be useful in artificially increasing the greenhouse effect on a planet, which could have applications in terraforming a planet to increase its suitability for life (Marinova et al. 2005; Dicaire et al. 2013). The detectability of CFCs for a planet orbiting a white dwarf host star was examined by Lin et al. (2014), who focused specifically on CCl_3F (known as CFC-11) and CF_4 (known as CFC-14) because they both show strong absorption features in the IR. Lin et al. (2014) estimated that CFCs at abundances 10 times greater than present-day Earth could be detected in a white dwarf system by the James Webb Space Telescope (JWST) with ~1.7 days of observing time.

Here we calculate detectability limits of CFCs for an Earth-sized planet orbiting an M-dwarf star. Such systems are likely targets for characterization by upcoming space missions such as the JWST or mission concepts such as LUVOIR, the Habitable Exoplanet (HabEx; Gaudi et al. 2018), Origins (Meixner et al. 2019), or the Large Interferometer for Exoplanets (LIFE; LIFE collaboration et al. 2021; Quanz et al. 2019), in addition to large ground-based observatories such as Extremely Large Telescopes (ELTs; Quanz et al. 2015; Snellen et al. 2015). We focus on the detectability of CFC-11 (CCl_3F) and CFC-12 (CCl_2F_2), which are two of the most abundant CFCs in Earth's atmosphere with elevated levels that have persisted despite the Montreal Protocol. Our model simulations are constrained to planets within the habitable zone of the host star, which represents the circumstellar region where a terrestrial planet could sustain surface liquid water (Kasting et al. 1993; Kopparapu et al. 2013). Planets within the habitable zone of low-mass stars are expected to fall into synchronous rotation, so that one side of the planet experiences perpetual day with the other side in perpetual night. We use a three-dimensional general circulation model (GCM) to calculate the equilibrium climate state for such synchronously rotating habitable planets at Earth-like and elevated abundances of CFCs. We then use the steady-state output from these GCM simulations to calculate synthetic IR spectra to show that absorption features of these CFCs could be detectable with missions such as the JWST and Origins.

2. Climate Modeling

The climate simulations in this study are conducted with the model called resolving orbital and climate keys of Earth and extraterrestrial environments with dynamics (ROCKE-3D; Way et al. 2017). ROCKE-3D is a GCM that has been developed by the NASA Goddard Institute for Space Studies for the study of planetary habitability. ROCKE-3D has been used to understand the climate of ancient Venus (Way et al. 2016; Way and Del Genio 2020), to explore possible habitable climates for specific exoplanets (Kane et al. 2018; Del Genio et al. 2019; Fauchez et al. 2020), and to constrain the dependences of general habitability limits on planetary properties (Fujii et al. 2017; Way & Georgakarakos 2017; Checklair et al. 2019; Colose et al. 2019; Olson et al. 2020; Salazar et al. 2020). Our configuration of ROCKE-3D assumes aquaplanet (i.e., ocean-covered) conditions with a 1 bar atmosphere composed of N_2 and H_2O with 400 ppm CO_2. We used a "slab" ocean with a fixed 50 m depth and a present-day Earth q-flux parameterization of oceanic energy transport. The use of a slab ocean significantly reduces computational time, although the use of a dynamic ocean can cause differences in surface temperature by a few degrees (Colose et al. 2021). The model
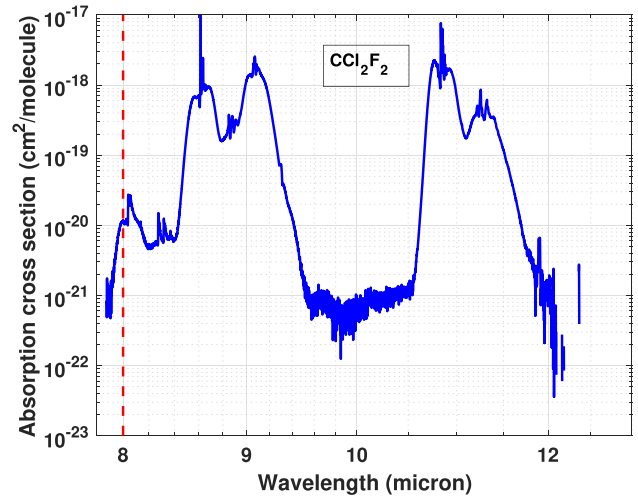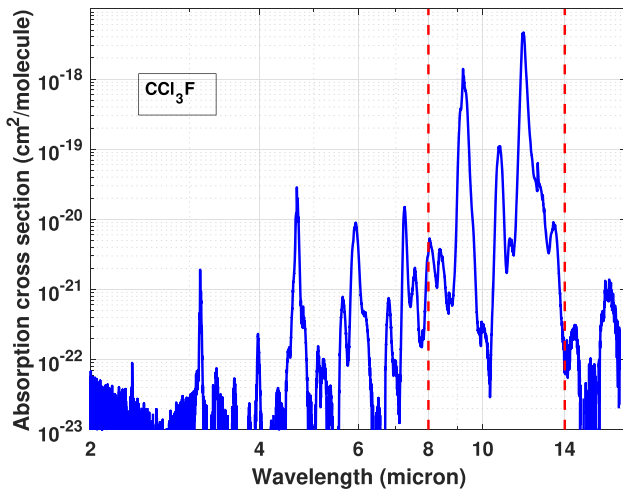
Figure 1. The absorption cross sections for CFC-11 (left) and CFC-12 (right) show the strongest features within a 8–14 μm window (dashed red lines) with one major peak between 8 and 10 μm and a second between 10 and 14 μm. Cross sections are from the HITRAN database with 0.003 μm resolution at 300 K (Sharpe et al. 2004; Harrison 2015; Gordon et al. 2021).

includes 40 vertical layers and a $4° \times 5°$ horizontal resolution. We assume a planet with zero obliquity that has the mass and gravitational acceleration of Earth. A more thorough discussion of the model configuration, including details of the radiative transfer methods, is provided by Colose et al. (2021), while a broader technical description of ROCKE-3D is given by Way et al. (2017).

Here we perform ROCKE-3D simulations of an Earth-sized planet in synchronous rotation around a 3300 K and TRAP-PIST-1 host stars with increased abundances of atmospheric CFC-11 and CFC-12. These species are included in ROCKE-3D as part of the Earth system model. They have strong absorption bands in the mid-IR part of the spectrum (Figure 1); however, this part of the IR spectrum is dominated by several other greenhouse gases such as CO_2, H_2O, and CH_4 (Figure 2) that could make a detection of CFCs difficult with upcoming observatories. In Section 3 we discuss the detectability of CFC-11 and CFC-12 in detail. We focus on these two particular systems because they are characteristic of systems likely to actually be studied by missions such as the JWST and Origins, in which CFCs could actually be detectable.

Our model experiments consist of four simulations conducted with different atmospheric abundances of CFC-11 and CFC-12. Both of these are potent greenhouse gases with an average lifetime of ∼55 yr for CFC-11 and ∼140 yr for CFC-12 in the Earth-Sun system (Seinfeld & Pandis 2006). The 0× case contains no CFCs and provides a reference control case for comparison. The 1× case includes 0.225 ppb CFC-11 and 0.515 ppb CFC-12, which are the present-day abundances of these CFCs on Earth.[11] The subsequent 2× and 5× cases contain CFC-11 and CFC-12 abundances that have been increased by 2 and 5 times, respectively. These elevated CFC abundances are realistic projections, shown in Figure 3, that could have occurred on Earth if the Montreal Protocol had been ineffective (see Young et al. 2021).

The CFC abundance is fixed in the model, with no sinks or sources due to chemistry. On Earth, the sources of CFC-11 and CFC-12 are industrial sites at the surface, while the only sinks
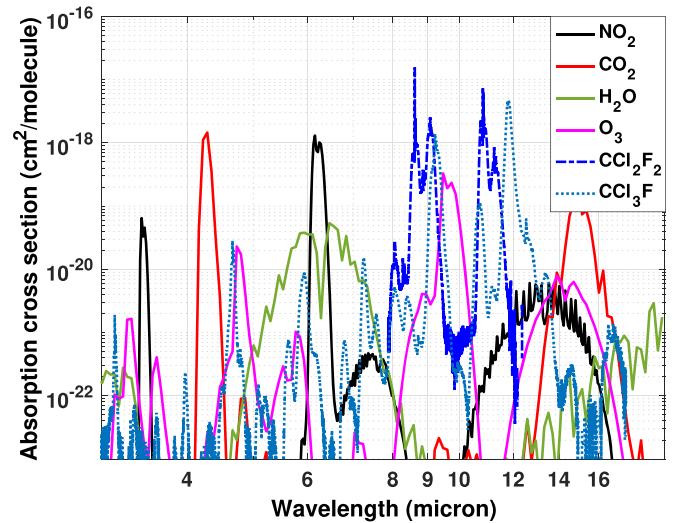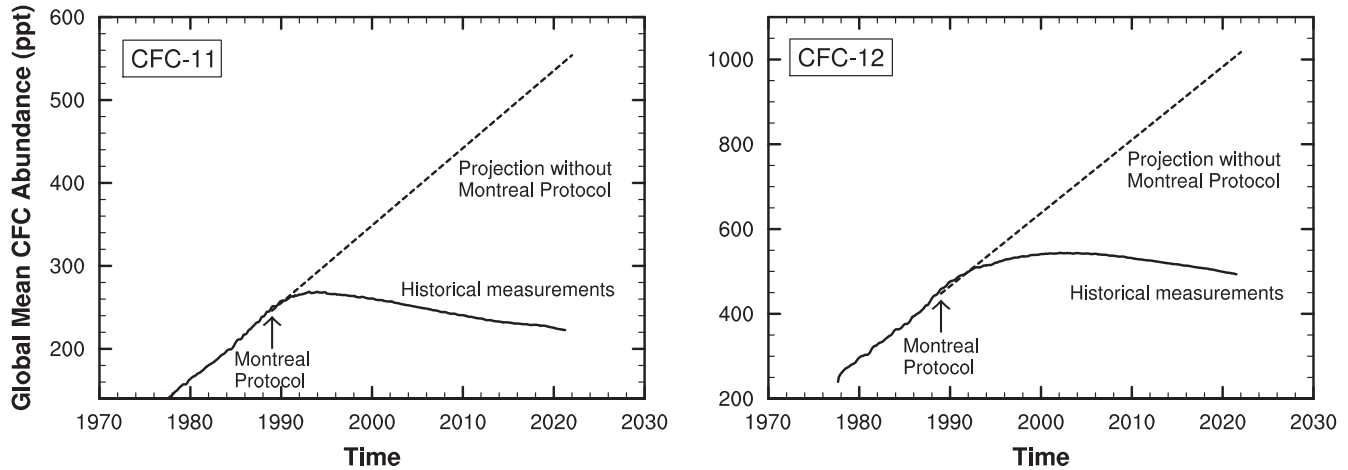

Figure 2. Examples of other atmospheric gases on Earth that have overlapping absorption features with CFC-11 and CFC-12 within the 8–14 μm window. Cross sections are from the HITRAN database with 0.003 μm resolution at 300 K (Sharpe et al. 2004; Harrison 2015; Gordon et al. 2021, 2022).

occur when the CFCs rise into the stratosphere and are photolyzed at wavelengths between 185 and 210 nm. This results in the relatively long atmospheric lifetimes of CFC-11 and CFC-12 on Earth. Planets orbiting M dwarfs tend to receive even less incident shortwave radiation on average, so the lifetime of CFCs may be even longer. This study presents a set of steady-state calculations with fixed CFC abundances that are intended to constrain the order of magnitude of detectability, but further studies with a coupled chemistry-climate GCM would provide more robust constraints on plausible upper limits for the abundance and lifetime of CFCs.

We consider two planet-star system configurations, both of which are motivated by previous studies of planetary habitability using GCMs. The first configuration uses a climate configuration for TRAPIST-1e that was defined and studied in previous model intercomparisions (Fauchez et al. 2020, 2021). The second configuration uses a climate configuration for a planet in the habitable zone of a 3300 K host star that has been

Figure 3. Historical measurements of CFC-11 (left) and CFC-12 (right) show a sharp decline that correlates with the adoption of the Montreal Protocol (solid curves). A linear projection shows that CFC abundances of twice as high or greater than today could have been possible if this treaty had not been effective (dashed lines). CFC data are from the National Oceanic and Atmospheric Administration (NOAA) Global Monitoring Laboratory.

examined in previous studies (Kopparapu et al. 2017; Colose et al. 2021).

2.1. TRAPPIST-1 Host Star

The seven-planet TRAPPIST-1 system (Gillon et al. 2017) is a target of particular interest by the JWST, ELTs, and other future missions, with TRAPPIST-1e orbiting within the star's liquid-water habitable zone. Climate modeling studies of the TRAPPIST-1 planets seek to explore possible habitable, and uninhabitable, spectral signatures that could be identified in future attempts at spectral atmospheric characterization (e.g., Wolf 2017; Turbet et al. 2018; Fauchez et al. 2019; Sergeev et al. 2020; Kane et al. 2021; May et al. 2021). Recently, the TRAPPIST-1 Habitable Atmosphere Intercomparison (THAI) workshop established a framework for comparing the capabilities of models to simulate the climate of TRAPPIST-1e, with four GCMs (including ROCKE-3D and ExoCAM) used as the basis for this intercomparison (Fauchez et al. 2020, 2021). This process focused on four specific scenarios for the atmosphere of TRAPPIST-1e, which showed general agreement but also revealed some differences in the mean and time-varying states of each of the models. The use of modeling protocols and intercomparisons such as THAI provide a systematic approach toward the use of climate models for understanding exoplanet habitability.

For the first system in this study, we use the same ROCKE-3D configuration as was used for THAI by Fauchez et al. (2020) to investigate the detectability of CFCs on TRAPPIST-1e. The model setup assumes a 2590 K BT-Settl spectrum for the TRAPPIST-1 host star with with a luminosity of $0.000553L_\odot$ and a mass of $0.0898M_\odot$. The planet TRAPPIST-1e is assumed to be in synchronous rotation with a rotational and orbital period of 6.1 days, an incident stellar flux of $0.662F_\oplus$, a mass of $0.772M_\oplus$, and a radius of $0.910R_\oplus$ (see Table 1 by Fauchez et al. 2020). The model is configured according to the THAI Hab1 case, which includes a 1 bar atmosphere composed of N_2 with 400 ppm CO_2 and H_2O as a variable gas, as with the 3300 K cases described next. These simulations also use a fixed slab ocean, which remains consistent with the THAI simulations. Our simulations of TRAPPIST-1e began with 300 K isothermal initial conditions and ran for 9800 model orbits to reach a statistically steady

state, and our analysis focuses on an average of the final 1000 orbits. (Note that this long integration time is required when using the ROCKE-3D GCM to simulate synchronously rotating planets with short orbital periods.)

2.2. 3300 K Host Star

A recent study by Colose et al. (2021) used ROCKE-3D to calculate the limits of the inner edge of the habitable zone for Earth-sized planets in synchronous rotation around low-mass stars with effective temperatures ranging from 4500 to 2600 K. The stellar spectra used by Colose et al. (2021) were the same set of BT-Settl model spectra from a previous study of the inner edge of the habitable zone by Kopparapu et al. (2017) that used the ExoCAM GCM. Likewise, the simulations performed by Colose et al. (2021) with ROCKE-3D used the same values of planetary rotation rate and orbital distance as were used in the simulations by Kopparapu et al. (2017), which were calculated for each host star to remain consistent with Kepler's laws. This approach allowed Colose et al. (2021) to identify systematic differences between the two GCMs when calculating the inner edge of the habitable zone, which included a comparison of both models configured with a fixed-depth slab ocean. Although some differences arose due to each model's parameterization of cloud formation, the two models generally provided similar constraints on the inner edge of the habitable zone.

For the second system in this study, we use the same ROCKE-3D configuration as was used by Colose et al. (2021) to investigate the detectability of CFCs on planets in the habitable zone of a low-mass star. We focus a set of our simulations on a 3300 K BT-Settl host star with a luminosity of $0.00972L_\odot$ and a mass of $0.249M_\odot$. The choice of a 3300 K host star falls in the middle of the range of stellar effective temperatures considered by Colose et al. (2021) and Kopparapu et al. (2017). The dynamical state of the atmosphere of synchronously rotating planets also changes with its rotation rate, and thus with its distance from the star. An analysis of the Kopparapu et al. (2017) simulations by Haqq-Misra et al. (2018) showed that the 4500–3300 K cases reside in a "slow rotation" regime with strong heating and convection beneath the planet's substellar point and a much colder night side, whereas the 2600 K and 3000 K cases fall into "rapid" and
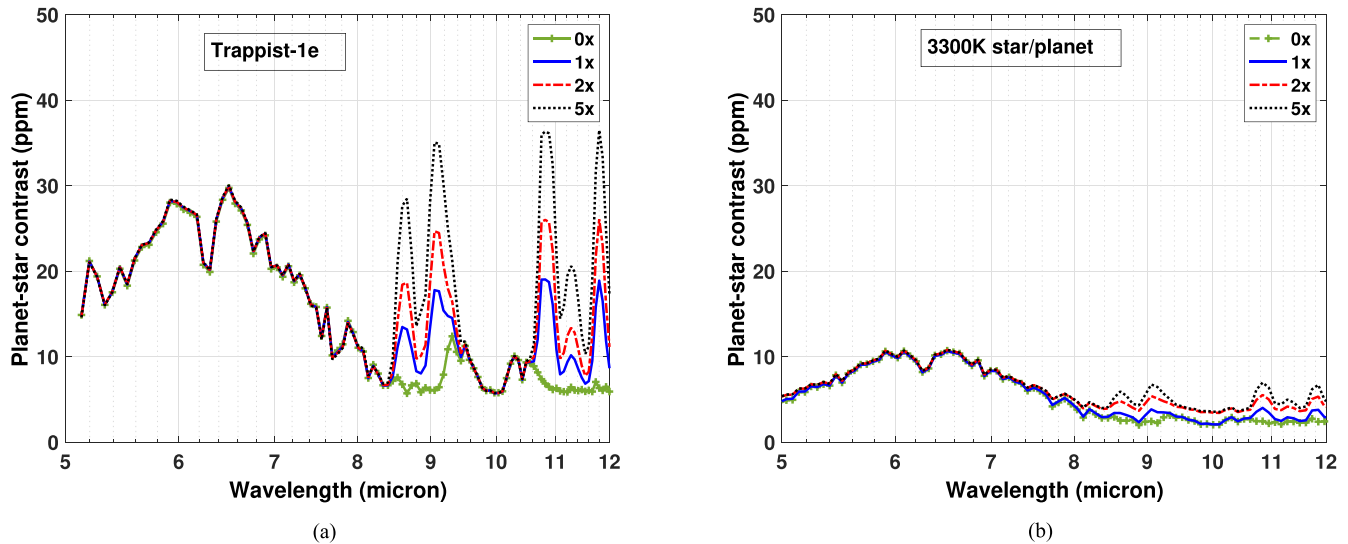
Figure 4. Transit spectra for TRAPPIST-1e (left) and an Earth-like planet around a 3300 K host star (right), showing the spectral features of CFC-11 and CFC-12 for the $0\times$, $1\times$, $2\times$, and $5\times$ scenarios. The features are more pronounced around Trappist-1 because of the smaller size of the star. The planets are in the respective habitable zones of their host stars, and the 3300K system is kept at a distance of 5 pc from the solar system (TRAPPIST-1 is at a distance of 12.4 pc).

"intermediate" rotation conditions, respectively, with enhanced zonal energy transport that leads to a warmer planetary night side. The slow rotation regime in particular has been widely examined by others (e.g., Joshi et al. 1997; Joshi 2003; Merlis & Schneider 2010; Carone et al. 2014; Kopparapu et al. 2016; Turbet et al. 2016; Del Genio et al. 2019). The choice of a 3300 K host star in this study yields a commonly expected atmospheric state for a synchronously rotating terrestrial planet orbiting within in the habitable zone.

For this 3300 K host star, we select a single case of an Earth-sized planet in synchronous rotation with a rotational and orbital period of 22.12 days and an incident stellar flux of $1.029 F_\oplus$ (see Table 1 by Kopparapu et al. 2017). This scenario places the planet near the inner edge of the conventional liquid-water habitable zone of its host star (Kasting et al. 1993; Kopparapu et al. 2013), but at a distance where the planet retains habitable surface conditions and does not show signs of a moist or runaway greenhouse (Kopparapu et al. 2017; Colose et al. 2021). This choice of orbital position is consistent with the assumption in our model that water vapor is the primary atmospheric condensible; by contrast, a terrestrial planet farther toward the outer edge of the habitable zone would reside in conditions where carbon dioxide condensation also occurs. This particular model configuration also shows a minimal difference between the use of a fixed slab ocean compared to a dynamic ocean, as shown in the comparison by Colose et al. (2021). Our simulations of this 3300 K scenario began with 300 K isothermal initial conditions and ran for 410 model orbits to reach a statistically steady state, and our analysis focuses on an average of the final 100 orbits. (Note that synchronously rotating systems in the slow rotation regime require a much shorter integration time using ROCKE-3D than planets in a rapid rotation regime.)

3. Synthetic Spectra

Our GCM simulations give steady-state solutions for atmospheres with fixed abundances of CFC-11 and CFC-12, which can be used to identify the strength of potentially observable spectral features. We use the calculated outgoing IR

flux values, cloud opacity, and greenhouse-gas mixing ratio values from our GCM simulations as input to the Planetary Spectrum Generator (PSG; Villanueva et al. 2018) to calculate synthetic spectra and assess limits of detectability. PSG is an online radiative transfer software that can be used to compute planetary spectra (atmospheres and surfaces) for various objects of the solar system and beyond. It includes a wide range of wavelengths (UV, visible, near-IR, IR, far-IR, THz, submillimeter, and radio) from any observatory, orbiter, or lander and also includes a noise calculator. In this work, we use a PSG add-on called Global Exoplanet Spectra (GlobES), which allows the user to ingest data from a variety of GCMs to accurately synthesize planetary spectra that are then computed with PSG. GlobES has been used for climate studies of TOI-700 day—the first habitable-zone terrestrial size planet discovered with TESS (Suissa et al. 2020).

We consider the GCM calculations in Section 2 for planets around TRAPPIST-1 and a 3300 K host star. For our synthetic spectra calculations, we use updated parameters for TRAP-PIST-1 and TRAPPIST-1e from Agol et al. (2021). (Although our GCM simulations use older parameters from Grimm et al. 2018, this discrepancy does not have any quantifiable impact on our results.) The reason for focusing on M dwarfs is that near-term atmospheric characterization telescope missions focus on planets around M dwarfs, and their instruments will operate in the IR part of the electromagnetic spectrum. Likewise, as mentioned in earlier sections, CFC-11 and CFC-12 have dominant absorption in the IR, so the confluence of instruments operating in the IR region and the corresponding strong absorption of CFCs makes M-dwarf planets ideally suited for studying CFC detectability. Here we focus on generating the transit spectra of planets around M dwarfs, and we then estimate the observing time needed to detect the dominant CFC features with the JWST and Origins.

Figure 4 shows transit spectra for TRAPPIST-1e and an Earth-like planet around 3300 K star, both with $0\times$, $1\times$, $2\times$, and $5\times$ Earth-level abundances of CFC-11 and CFC-12. The strongest absorption features are between the 8 and 12 μm range. We focus our detectability estimates within this region. As expected, higher amounts of CFCs increase the transit
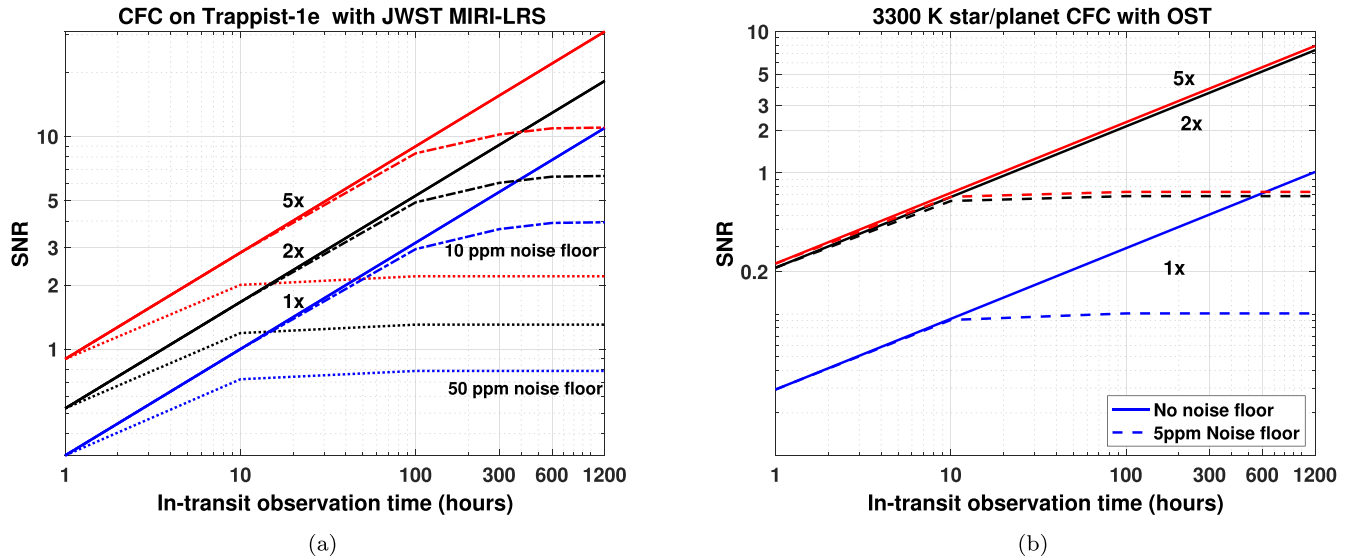
Figure 5. In-transit time (i.e., no overheads) S/N estimates as a function of CFC concentration for TRAPPIST-1e (left) and a planet around a 3300K star (right). The left panel shows JWST MIRI-LRS simulated observations of TRAPPIST-1e at observing times ranging from 1 to 1200 hr with a lower limit of the noise floor of 10 ppm and a higher limit of 50 ppm. With an optimistic 10 ppm noise floor, current Earth-level CFCs ($1\times$) could be detectable with an S/N $\sim$ 3 in about $\sim$100 hr of JWST MIRI-LRS in-transit observations. Past Earth-level ($2\times$) CFCs could be detectable on TRAPPIST-1e with an S/N $\sim$ 5 for the same amount of time. However, a very conservative 50 ppm noise floor would render even a $5\times$ present Earth-level CFC abundance challenging to detect. The right panel shows simulated observations with Origins for a planet around a 3300 K star, with a noise floor of 5 ppm. Despite the lower noise floor, detection of CFCs around this star would be difficult due to the larger size of the star.

depth, which is represented as the planet-to-star contrast ratio in parts per million (ppm) on the y-axis. The depth of the 8–14 μm features for TRAPPIST-1e is higher than that of a planet around a 3300 K star because the stellar host is correspondingly smaller (TRAPPIST-1 is just slightly larger than Jupiter), which would enable a relatively larger surface area of the star to be transited by the planet and would therefore increase the transit depth. This suggests that CFC absorption features might be easier to detect around late M dwarfs than the earlier ones.

To estimate the signal-to-noise ratio (S/N) for detecting these CFC features, we kept the TRAPPIST-1e planet at a star-planet separation of 0.029 3 au and at a distance of 12.4 pc. We used the TRAPPIST-1e planet parameters from Grimm et al. 2018 for our GCM simulations as done in THAI (Fauchez et al. 2020). For the planet around a 3300 K star, we kept the planet at 0.1 au, corresponding to the habitable zone for this star, and at a distance of 5 pc from Earth. Any S/N calculations can be qualitatively scaled to other distances based on our results for this star type. We have calculated the S/N by subtracting the $0\times$ case with no CFCs from the $1\times$, $2\times$, and $5\times$ cases and dividing the result with the noise, all within a wavelength range of the instrument under consideration. This method evaluates the S/N with respect to the $0\times$ level of the observed spectra.

Figure 5 (left) shows the S/N values for $1\times$ (blue), $2\times$ (black), and $5\times$ (red) CFC versus in-transit observation time in hours (i.e., no overheads) with the JWST Mid-Infrared Instrument low-resolution spectrometer (MIRI-LRS) using a resolution $R = 50$. Two levels of noise floors are shown as well: 10 ppm (dashed) and 50 ppm (dotted). We note that these noise floors are applied to multiple coadded observations, and the 50 ppm floor is therefore expected to be very conservative. With a 10 ppm noise floor, concentrations at the current Earth level ($1\times$, dashed blue) can be detectable with an S/N $\sim$ 3 in $\sim$100 hr. While this may not be a robust detection, this could hint at a possible feature for further observations. However, the features of a $2\times$ CFC level, which might have been Earth's

current CFC level without the Montreal protocol, would be detectable with an S/N $\sim$ 5 with the same amount of time. We would be able to detect the features of a planet with a $5\times$ CFC level (dashed red) with an S/N $\sim$ 10 in 100 hr of JWST MIRI-LRS time on TRAPPIST-1e. However, if the noise floor is set at 50 ppm, then even the $5\times$ CFC features would not be detectable with a reliable S/N, regardless of the JWST MIRI-LRS observation time. While upper limits can be placed, these limits will not be robust to make any meaningful analysis.

Figure 5 (right) shows similar S/N calculations for CFC on an Earth-like planet around a 3300 K host star using Origins. The system is located at 5 pc from Earth, which is intended to provide an optimal scenario for calculating CFC detection limits for Origins. There are about 60 stars within 5 pc, most of which are M dwarfs with about half in binaries, all of which are on the Breakthrough Listen target list (Isaacson et al. 2017). The spectral features are muted (see Figure 4, right) owing to a larger star, and the S/N values are lower than for TRAPPIST-1e for the present Earth-level case. However, higher CFC concentrations generate much higher S/N values. For the $2\times$ and $5\times$ CFC cases, an S/N $\sim$ 5 can be achieved with $\sim$600 hr of Origins observing time.

Note that the estimated integration times only take into account in-transit times. The real observation times including overhead would likely be two or three times longer. Moreover, no instrument noise systematics were considered in our JWST simulations, which only include pure white noise (i.e., noise that decreases with $1/\sqrt{photons}$). The real noise will decrease at a slower rate and will therefore increase the required number of transits to achieve 3 or 5σ. Furthermore, for long integration times over a large aperture like that of the JWST, instrument systematics are expected to lead to a noise floor that is at a level of noise that cannot be reduced by adding more observations, as shown in Figure 5 (Fauchez et al. 2019).

As mentioned above, $\sim$100 hr of JWST MIRI-LRS observing time are needed to detect present Earth-level CFCs

on TRAPPIST-1e with a noise floor of 10 ppm. Almost every transit in the JWST mission lifetime would need to be observed to reach ∼100 hr of in-transit time. There are ∼100 transits observable between 2022 June and 2028 July; this is technically longer than the nominal mission lifetime of 5.5 yr of the JWST, but NASA now estimates that JWST "should have enough propellant to allow support of science operations in orbit for significantly more than a 10 yr science lifetime."[12] TRAPPIST-1e is likely going to remain the best target for such observations in the foreseeable future, so such an investment would be an expensive but potentially highly rewarding program.

Here, we have only calculated whether the effects of CFCs might be detectable at all and what its form would be, and not whether they can be unambiguously retrieved from a real spectrum given realistic ambiguities of the host planet's atmospheric structure and composition, and host star's intrinsic spectrum. We leave an analysis of these complexities to a future study.

In summary, the absorption features of CFC-11 and CFC-12 could potentially be detectable by upcoming missions such as the JWST, depending on the noise floor levels. Present or past Earth-like abundances of CFCs could be detected with observing times of ∼100–300 hr at an S/N $\gtrsim$3–5. Large observing programs have been conducted previously, such as ∼400 hr for the Hubble Ultra Deep Field (Beckwith et al. 2006) or ∼900 hr for the CANDLES galaxy evolution survey (Grogin et al. 2011), so this requirement remains plausible. Moreover, such large observing programs are smaller than the estimates for biosignatures in a modern Earth-like atmosphere on TRAPPIST-1e (Fauchez et al. 2019; Lustig-Yaeger et al. 2019), i.e., ∼600 hr for O_3 detection at 9.6 μm or ∼800 hr for O_2 at 6.4 μm, with CH_4 and H_2O being undetectable in this scenario. An interesting point here is that the time needed to detect some present-Earth biosignature gases (∼600 hr) is longer than the observing time needed to detect present-Earth abundances of CFCs (∼300 hr) with the JWST. Furthermore, any attempt at characterizing spectral technosignatures would be conducted in tandem with a more general effort to characterize a planet's atmosphere and identify any potential biosignatures. Calculations such as those presented in this paper are useful in determining observability thresholds for detecting particular technosignatures, such as CFCs, which can aid in the development of observing strategies as well as motivate the design of new technology for future missions.

4. Discussion

Halocarbons such as CFC-11 and CFC-12 are industrial compounds on Earth and thus could be evidence of extraterrestrial technology if observed in an exoplanet atmosphere. In the event of such an observation in exoplanet spectra, any absorption features claimed to be technosignatures would need to be examined against nontechnological and nonbiological alternatives. On Earth, there are no known abiotic or nonanthropogenic sources of CFC-11 or CFC-12 (Seinfeld & Pandis 2006), likely because such molecules are thermodynamically challenging to produce; however, this does not necessarily mean that CFC-11 or CFC-12 could not be generated on an exoplanet through nontechnological means.

For example, other halocarbon species can be emitted to the atmosphere by phytoplankton, although these tend to be short lived (Lim et al. 2017). This is an instance of a more general problem in biosignature science, as identifying false positives that occur on exoplanets but not on Earth is a challenging task. Nevertheless, advancing the science of technosignatures will require evaluating such false positives for technosignatures such as CFCs, just as biosignature science continues to evaluate false-positive spectral signatures for habitability.

The calculations presented in this study indicate that CFCs could potentially be detectable by upcoming missions and future mission concepts given noise floor constraints, even at present-day Earth levels. The detection of absorption features within the 8–14 μm region, and subsequent identification of CFCs as the source of these features, will remain challenging, and future work will be needed to improve constraints on the detectability of CFCs for specific targets as observed by the JWST, Origins, or other missions. This study focused on the detectability of two M-dwarf systems that could plausibly be observed by the JWST or Origins, but future work could examine the possible detectability of CFCs in the atmospheres of habitable planets around solar-type stars with other mission concepts, such as LIFE.

We note that our study has focused on the concept of "detectability" for CFCs, and the actual detections of absorption features within the 8–14 μm region would not themselves be sufficient evidence to conclude the presence of CFCs in an exoplanet atmosphere. For an atmospheric composition like present-day Earth, CFCs may show some unique spectral features that help distinguish it from other gases (Figure 2), but other molecules such as CH_4, NH_3, CO, H_2S, and PH_3 also have absorption features that overlap with those of CFC-11 and CFC-12. Resolving any ambiguity regarding the identity of absorbing species will require further observations at other wavelengths that resolve additional absorption features. Theoretical modeling can also help to provide constraints on possible false-positive (and false-negative) scenarios for detecting CFCs in the atmospheres of exoplanets.

One limitation of this modeling study is that CFC abundances were assumed to be fixed and scaled without consideration of atmospheric chemistry. The use of a coupled chemistry-climate model would allow for a more self-consistent prediction of CFC abundances that could be sustained in the atmosphere, which would depend on the atmospheric composition as well as on the stellar spectrum. Our GCM cases also assumed a uniform distribution of CFCs across the atmosphere, which assumes that localized sources or sinks of CFC production are well mixed over time. However, scenarios in which strong, localized, and continuous sources and sinks of CFCs dominate other sources and sinks on the planet would require further study with a coupled climate-chemistry model to more accurately constrain the detectability of CFCs.

It is worth asking whether it is even reasonable to consider the detectability of planets with CFC abundances much greater than those on Earth today. Governments on Earth have banned the use of CFCs that could deplete ozone, while the threat of exacerbating climate change keeps our civilization from allowing long-lived radiatively active CFCs to accumulate in significant quantities. Such risks could also motivate extraterrestrial civilizations to minimize use of CFCs, although this is strongly dependent on the details of the climate needs of this

---

[12] https://blogs.nasa.gov/webb/2021/12/29/nasa-says-webbs-excess-fuel-likely-to-extend-its-lifetime-expectations/

species, the atmospheric composition of the planet, and many assumptions about the long-term aims and coordination of the species. For instance, the species might be incapable of preventing the buildup (because it is insufficiently organized or motivated to), indifferent to the buildup (because it has no important effects on the planet or because they are unaware of those effects), or causing the buildup deliberately (because it wishes to warm the planet, perhaps).

This study focused on planets in M-dwarf systems because such systems are likely to be characterized by upcoming missions, and the steady-state photochemistry on such planets will differ due to lower reaction rates for many atmospheric constituents. For example, planets orbiting K- and M-dwarf stars can accumulate O_3 more easily (e.g., Segura et al. 2010; Arney 2019), which could allow for CFCs to accumulate to higher levels than on Earth before causing environmental problems. Such scenarios should be considered in future work and should also be expanded to include a broad range of halocarbons beyond CFC-11 and CFC-12 only. Similarly, this study focused on the detectability limits of upcoming space missions, but future high-resolution ground-based spectroscopy facilities such as Extremely Large Telescopes (e.g., Cavarroc et al. 2006; Snellen et al. 2013; Kuhn & Berdyugina 2015; Lovis et al. 2017; Birkby 2018) may also be able to detect the presence of CFCs in exoplanet atmospheres.

We do not know the extent to which the specific CFCs produced on Earth would be prevalent elsewhere, even for extraterrestrial civilizations with similar industrial processes. The family of halocarbons is large, and much more work is needed to assess the detectability of a broader range of industrial molecules. This effort would be a step toward constructing a library of technosignatures for planning and interpreting future observations. But even such a library may be unable to identify industrial molecules that are chemically possible but have never been generated on Earth. Efforts to explore other possible industrial molecules, as well as their spectral signatures, could also help to constrain the use of halocarbons in general as technosignatures.

5. Conclusion

The CFCs are a notable example of a technosignature on Earth, and the detection of CFCs on a planet like TRAPPIST-1e would be difficult to explain through any biological or geologic features we know of today. Our civilization continues along a path of growth in both population and energy consumption, while we are only beginning to understand the extent to which our technology could be detectable at astronomical distances. Continued exploration of how the past, present, and future of civilization will affect Earth's detectability remains an important objective for understanding the prevalence of biosignatures and technosignatures in our galaxy.

In this study, we have shown that with the launch of the JWST, humanity may be very close to an important milestone in SETI: one where we are capable of detecting from nearby stars not just powerful, deliberate, transient, and highly directional transmissions like our own (such as the Arecibo Message), but consistent, passive technosignatures of the same strength as our own. Note that this is not a symmetric situation: the detectability of CFCs in an Earth-like planet's atmosphere is strongly dependent on the radius and spectrum of the host star, and the TRAPPIST-1 system in particular is extremely favorable in this regard. Even if Earth were seen to transit from

that system, the Sun's large radius and Earth's orbital distance mean that the JWST would not detect CFCs around Earth from the distance of TRAPPIST-1.

In the next few decades, at least two of Earth's passive technosignatures, radio emissions and atmospheric pollution, would be detectable by our own technology around the nearest stars. It is possible that other plausible atmospheric technosignatures will prove even more detectable once their signal strengths have been calculated. We conclude that atmospheric technosignatures are at least as promising as communicative, radio technosignatures in this regard, especially since they can be searched for concurrently with biosignatures.

ORCID iDs

Jacob Haqq-Misra ● https://orcid.org/0000-0003-4346-2611
Ravi Kopparapu ● https://orcid.org/0000-0002-5893-2471
Thomas J. Fauchez ● https://orcid.org/0000-0002-5967-9631
Jason T. Wright ● https://orcid.org/0000-0001-6160-5888
Manasvi Lingam ● https://orcid.org/0000-0002-2685-9417

References

Agol, E., Dorn, C., Grimm, S. L., et al. 2021, PSJ, 2, 1
Arney, G. N. 2019, ApJL, 873, L7
Arnold, L. 2005, ApJ, 627, 534
Beckwith, S. V., Stiavelli, M., Koekemoer, A. M., et al. 2006, AJ, 132, 1729
Benneke, B., Wong, I., Piaulet, C., et al. 2019, ApJL, 887, L14
Birkby, J. L. 2018, in Handbook of Exoplanets, ed. H. Deeg & J. Belmonte (Cham: Springer), 16
Bracewell, R. N. 1960, Natur, 186, 670
Brown, D., Brownrigg, R., Haley, M., & Huang, W. 2012, UCAR/NCAR Computational and Information Systems Laboratory, 10, D6WD3XH5, 10
Campbell, J. B. 2006, in IAU Coll. 200, Direct Imaging of Exoplanets: Science & Techniques, ed. C. Aime & F. Vakili (Cambridge: Cambridge Univ. Press), 247
Carone, L., Keppens, R., & Decin, L. 2014, MNRAS, 445, 930
Carrigan, R., Jr. 2009, in ASP Conf. Ser. 420, Bioastronomy 2007: Molecules, Microbes and Extraterrestrial Life, ed. K. Meech (San Francisco, CA: ASP), 415
Catling, D. C., Krissansen-Totton, J., Kiang, N. Y., et al. 2018, AsBio, 18, 709
Cavarroc, C., Boccaletti, A., Baudoz, P., Fusco, T., & Rouan, D. 2006, A&A, 447, 397
Charbonneau, D., Brown, T. M., Noyes, R. W., & Gilliland, R. L. 2002, ApJ, 568, 377

Checlair, J. H., Olson, S. L., Jansen, M. F., & Abbot, D. S. 2019, ApJL, 884, L46
Chipperfield, M. P., Bekki, S., Dhomse, S., et al. 2017, Natur, 549, 211
Cocconi, G., & Morrison, P. 1959, Natur, 184, 844
Colose, C. M., Del Genio, A. D., & Way, M. J. 2019, ApJ, 884, 138
Colose, C. M., Haqq-Misra, J., Wolf, E. T., et al. 2021, ApJ, 921, 25
Del Genio, A. D., Way, M. J., Amundsen, D. S., et al. 2019, AsBio, 19, 99
Dicaire, I., Forget, F., Millour, E., et al. 2013, in 64th Int. Astronautical Congress, IAC-13 (Beijing: IAF), 19180, https://iafastro.directory/iac/paper/id/19180/abstract-pdf/IAC-13,D3,3,10,x19180.brief.pdf?2013-04-05.11:45:16
Dyson, F. J. 1960, Sci, 131, 1667
Eyring, V., Cionni, I., Bodeker, G. E., et al. 2010, ACP, 10, 9451
Fauchez, T. J., Turbet, M., Villanueva, G. L., et al. 2019, ApJ, 887, 194
Fauchez, T. J., Turbet, M., Wolf, E. T., et al. 2020, GMD, 13, 707
Fauchez, T. J., Turbet, M., Sergeev, D. E., et al. 2021, PSJ, 2, 106
Forgan, D. 2013, JBIS, 66, 144
Forgan, D. H., & Nichol, R. C. 2011, IJAsB, 10, 77
Freitas, R. A., Jr., & Valdes, F. 1980, Icar, 42, 442
Fujii, Y., Del Genio, A. D., & Amundsen, D. S. 2017, ApJ, 848, 100
Fujii, Y., Angerhausen, D., Deitrick, R., et al. 2018, AsBio, 18, 739
Gaudi, S. B., Seager, S., Mennesson, B., et al. 2018, arXiv:1809.09674
Gillon, M., Triaud, A. H., Demory, B.-O., et al. 2017, Natur, 542, 456
Gordon, I., Rothman, L., Hargreaves, R., et al. 2022, JQSRT, 277, 107949
Gordon, I. E., Rothman, L. S., Hargreaves, R., et al. 2022, JQSRT, 277, 107949
Grenfell, J. L. 2017, PhR, 713, 1
Grimm, S. L., Demory, B.-O., Gillon, M., et al. 2018, A&A, 613, A68
Grogin, N. A., Kocevski, D. D., Faber, S., et al. 2011, ApJS, 197, 35
Haqq-Misra, J., & Kopparapu, R. K. 2012, AcAau, 72, 15
Haqq-Misra, J., Kopparapu, R. K., & Schwieterman, E. 2020, AsBio, 20, 572
Haqq-Misra, J., Wolf, E. T., Joshi, M., Zhang, X., & Kopparapu, R. K. 2018, ApJ, 852, 67
Harrison, J. 2015, AMT, 8, 3197
Isaacson, H., Siemion, A. P., Marcy, G. W., et al. 2017, PASP, 129, 054501
Joshi, M. 2003, AsBio, 3, 415
Joshi, M., Haberle, R., & Reynolds, R. 1997, Icar, 129, 450
Kaltenegger, L. 2017, ARA&A, 55, 433
Kane, S. R., Ceja, A. Y., Way, M. J., & Quintana, E. V. 2018, ApJ, 869, 46
Kane, S. R., Jansen, T., Fauchez, T., Selsis, F., & Ceja, A. Y. 2021, AJ, 161, 53
Kasting, J. F., Whitmire, D. P., & Reynolds, R. T. 1993, Icar, 101, 108
Kipping, D., & Teachey, A. 2016, MNRAS, 459, 1233
Kopparapu, R., Arney, G., Haqq-Misra, J., Lustig-Yaeger, J., & Villanueva, G. 2021, ApJ, 908, 164
Kopparapu, R., Wolf, E. T., Arney, G., et al. 2017, ApJ, 845, 5
Kopparapu, R., Wolf, E. T., Haqq-Misra, J., et al. 2016, ApJ, 819, 84
Kopparapu, R. K., Ramirez, R., Kasting, J. F., et al. 2013, ApJ, 765, 131
Kovesi, P. 2015, arXiv:1509.03700
Kuhn, J. R., & Berdyugina, S. V. 2015, IJAsB, 14, 401
Lammer, H., Sproß, L., Grenfell, J. L., et al. 2019, AsBio, 19, 927
LIFE collaboration, Quanz, S. P., Ottiger, M., et al. 2021, arXiv:2101.07500
Lim, Y., Phang, S., Rahman, N. A., Sturges, W., & Malin, G. 2017, International Journal of Environmental Science and Technology, 14, 1355
Lin, H. W., Gonzalez Abad, G., & Loeb, A. 2014, ApJL, 792, L7
Lingam, M., & Loeb, A. 2017, MNRAS, 470, L82
Lingam, M., & Loeb, A. 2021, Life in the Cosmos: From Biosignatures to Technosignatures (Cambridge: Harvard Univ. Press) https://www.hup.harvard.edu/catalog.php?isbn=9780674987579
Loeb, A., & Turner, E. 2012, AsBio, 12, 290
Loeb, A., & Zaldarriaga, M. 2007, Journal of Cosmology and Astro-Particle Physics, 2007, 020

Lovis, C., Snellen, I., Mouillet, D., et al. 2017, A&A, 599, A16
Lustig-Yaeger, J., Meadows, V. S., & Lincowski, A. P. 2019, AJ, 158, 27
LUVOIR Team 2019, arXiv:1912.06219
Marinova, M. M., McKay, C. P., & Hashimoto, H. 2005, JGRE, 110, E03002
May, E., Taylor, J., Komacek, T., Line, M., & Parmentier, V. 2021, The, ApJL, 911, L30
Meadows, V. S., Reinhard, C. T., Arney, G. N., et al. 2018, AsBio, 18, 630
Meixner, M., Cooray, A., Leisawitz, D., et al. 2019, arXiv:1912.06213
Merlis, T. M., & Schneider, T. 2010, JAMES, 2, 13
NASA Technosignatures Workshop Participants 2018, arXiv:1812.08681
Olson, S. L., Jansen, M., & Abbot, D. S. 2020, ApJ, 895, 19
O'Malley-James, J. T., & Kaltenegger, L. 2019, ApJL, 879, L20
Owen, T. 1980, in Strategies for the Search for Life in the Universe (Berlin: Springer), 177
Quanz, S. P., Crossfield, I., Meyer, M. R., Schmalzl, E., & Held, J. 2015, IJAsB, 14, 279
Quanz, S. P., Absil, O., Angerhausen, D., et al. 2019, arXiv:1908.01316
Rose, C., & Wright, G. 2004, Natur, 431, 47
Salazar, A. M., Olson, S. L., Komacek, T. D., Stephens, H., & Abbot, D. S. 2020, ApJL, 896, L16
Schneider, J., Léger, A., Fridlund, M., et al. 2010, AsBio, 10, 121
Schwieterman, E. W., Kiang, N. Y., Parenteau, M. N., et al. 2018, AsBio, 18, 663
Seager, S., Schrenk, M., & Bains, W. 2012, AsBio, 12, 61
Segura, A., Walkowicz, L. M., Meadows, V., Kasting, J., & Hawley, S. 2010, AsBio, 10, 751
Seinfeld, J., & Pandis, S. 2006, Atmospheric Chemistry and Physics (2nd ed.; New York: John Wiley & Sons)
Sergeev, D. E., Lambert, F. H., Mayne, N. J., et al. 2020, ApJ, 894, 84
Sharpe, S. W., Johnson, T. J., Sams, R. L., et al. 2004, ApSpe, 58, 1452
Shklovskii, I. S., & Sagan, C. 1966, Intelligent life in the universe (San Francisco, CA: Holden-Day) Trans. by P. Fern
Snellen, I., de Kok, R., Birkby, J. L., et al. 2015, A&A, 576, A59
Snellen, I. A. G., de Kok, R. J., le Poole, R., Brogi, M., & Birkby, J. 2013, ApJ, 764, 182
Stevens, A., Forgan, D., & James, J. 2016, IJAsB, 15, 333
Suissa, G., Wolf, E. T., Kopparapu, R. K., et al. 2020, AJ, 160, 118
Tabor, E., & Loeb, A. 2021, arXiv:2105.08081
Tarter, J. C. 2007, HiA, 14, 14
Tsiaras, A., Waldmann, I. P., Tinetti, G., Tennyson, J., & Yurchenko, S. N. 2019, NatAs, 3, 1086
Turbet, M., Leconte, J., Selsis, F., et al. 2016, A&A, 596, A112
Turbet, M., Bolmont, E., Leconte, J., et al. 2018, A&A, 612, A86
Velders, G. J., Andersen, S. O., Daniel, J. S., Fahey, D. W., & McFarland, M. 2007, PNAS, 104, 4814
Villanueva, G. L., Smith, M. D., Protopapa, S., Faggi, S., & Mandell, A. M. 2018, JQSRT, 217, 86
Walker, S. I., Bains, W., Cronin, L., et al. 2018, AsBio, 18, 779
Way, M. J., & Del Genio, A. D. 2020, JGRE, 125, e2019JE006276
Way, M. J., Del Genio, A. D., Kiang, N. Y., et al. 2016, GeoRL, 43, 8376
Way, M. J., & Georgakarakos, N. 2017, ApJL, 835, L1
Way, M. J., Aleinov, I., Amundsen, D. S., et al. 2017, ApJS, 231, 12
Whitmire, D., & Wright, D. 1980, Icar, 42, 149
Wolf, E. T. 2017, ApJL, 839, L1
Wright, J. T. 2019, BAAS, 51, 39
Wright, J. T., Cartier, K. M. S., Zhao, M., Jontof-Hutter, D., & Ford, E. B. 2016, ApJ, 816, 17
Wright, J. T., Griffith, R. L., Sigurdsson, S., Povich, M. S., & Mullan, B. 2014, ApJ, 792, 27
Wright, J. T., Sheikh, S., Almár, I., et al. 2018, arXiv:1809.06857
Young, P. J., Harper, A. B., Huntingford, C., et al. 2021, Natur, 596, 384